CHEMISTRY
AN ASIAN JOURNAL

DOI: 10.1002/asia.201000506

Alternating and Diblock Donor–Acceptor Conjugated Polymers Based on Diindeno[1,2-*b*:2′,1′-*d*]thiophene Structure: Synthesis, Characterization, and Photovoltaic Applications

Chiu-Hsiang Chen, Yen-Ju Cheng,* Martin Dubosc, Chao-Hsiang Hsieh, Cheng-Che Chu, and Chain-Shu Hsu*[a]

Abstract: Pentacyclic diindeno[1,2-*b*:2′,1′-*d*]thiophene (**DIDT**) unit is a rigid and coplanar conjugated molecule. To the best of our knowledge, this attractive molecule has never been incorporated into a polymer and thus its application in polymer solar cells has never been explored. For the first time, we report the detailed synthesis of the tetra-alkylated **DIDT** molecule leading to its dibromo- and diboronic ester derivatives, which are the key monomers for preparation of **DIDT**-based polymers. Two donor–acceptor alternating polymers, poly(diindenothiophene-*alt*-benzothiadiazole) **PDIDTBT** and poly(diindenothiophene-*alt*-dithienylbenzothiadiazole) **PDIDTDTBT**, were synthesized by using Suzuki polymerization. Copolymer **PTDIDTTBT** was also prepared by using Stille polymerization. Although **PTDIDTTBT** is prepared through a manner of random polymerization, we found that the different reactivities of the dibromo-monomers lead to the resulting polymer having a block copolymer arrangement. With the higher structural regularity, **PTDIDTTBT**, symbolized as (thiophene-*alt*-**DIDT**)$_{0.5}$-*block*-(thiophene-*alt*-BT)$_{0.5}$, shows the higher degree of crystallization, stronger π–π stacking, and broader absorption spectrum in the solid state, as compared to its alternating **PDIDTDTBT** analogue. Bulk heterojunction photovoltaic cells based on ITO/PEDOT:PSS/polymer:$PC_{71}BM$/Ca/Al configuration were fabricated and characterized. **PDIDTDTBT**/$PC_{71}BM$ and **PTDIDTTBT**/$PC_{71}BM$ systems exhibited promising power-conversion efficiencies (PCEs) of 1.65% and 2.00%, respectively. Owing to the complementary absorption spectra, as well as the compatible structures of **PDIDTDTBT** and **PTDIDTTBT**, the PCE of the device based on the ternary blend **PDIDTDTBT**/**PTDIDTTBT**/$PC_{71}BM$ was further improved to 2.40%.

Keywords: copolymerization · donor–acceptor systems · photovoltaics · polymers · solar cells

Introduction

Over the past few years, a tremendous research effort has been made on all-solution processed polymer solar cells (PSCs) to realize low-cost, light-weight, large-area, and flexible photovoltaic devices. PSCs based on the concept of bulk heterojunction (BHJ) are the most widely adopted device architecture to ensure a maximum internal donor–acceptor (D–A) interfacial area for efficient charge separation.[1] To achieve the high efficiency of PSCs, the most critical challenge at the molecular level is to develop p-type conjugated polymers that simultaneously possess 1) sufficient solubility to guarantee solution processability and miscibility with an n-type material, 2) low bandgap (LBG) for strong and broad absorption spectrum to capture more solar photons, and 3) high hole mobility for efficient charge transport. The most effective approach to produce an LBG polymer is to incorporate electron-rich donor and electron-deficient acceptor segments along the conjugated-polymer backbone.[2] In this regard, extensive research has been made on the development of new electron-rich donor segments for p-type materials.[3] Fluorene-containing compounds represent an important class of aromatic system for photovoltaic applications, owing to their good hole-transport properties and feasibility for chemical modifications. The tricyclic 2,7-fluorene

[a] C.-H. Chen, Prof. Dr. Y.-J. Cheng, Dr. M. Dubosc, C.-H. Hsieh, Dr. C.-C. Chu, Prof. Dr. C.-S. Hsu
Department of Applied Chemistry
National Chiao Tung University
1001 Ta Hsueh Road, Hsin-Chu, 30010 (Taiwan)
E-mail: yjcheng@mail.nctu.edu.tw
cshsu@mail.nctu.edu.tw

Supporting information for this article is available on the WWW under http://dx.doi.org/10.1002/asia.201000506.

unit has been shown to serve as an excellent building block to construct D–A polymers with deep-lying HOMO energy levels, which are a crucial prerequisite to achieve high open-circuit voltages (V_{oc}) for PSCs.[4] One intrinsic drawback, however, is that fluorene-containing polymers usually possess relatively large optical bandgaps (>2 eV), which limit their ability to efficiently harvest sunlight and, thus, result in only moderate photocurrents. Structurally analogous to fluorene, tricyclic 4*H*-cyclopenta[2,1-*b*:3,4-*b*′]dithiophene (**CPDT**),[5] with a cyclopentadiene (CP) ring embedded between two thiophene rings, appears to be another useful electron-rich donor segment for LBG polymers.[6] Although **CPDT**-based D–A polymers have exhibited sufficiently low optical bandgaps, strong intermolecular interactions, and excellent hole mobilities, leading to very high short-circuit currents (J_{sc}); the V_{oc} values of the devices are generally lower than 0.65 V. A common structural feature of the current successful LBG conjugated polymers is that the donor segments are composed of multi-fused aromatic rings with forced planarity.[3] Forced planarization by covalently fastening adjacent aromatic units in the polymer backbone strengthens the parallel p-orbital interactions to elongate effective conjugation length and facilitate π-electron delocalization to provide an effective way to reduce the band gap.[7] Moreover, coplanar geometries and rigid structures can suppress the rotational disorder around interannular single bonds and lower the reorganization energy, which, in turn, enhances the intrinsic charge mobility.[8] These analyses inspired us to integrate the core structures of fluorene and **CPDT** into a single molecular entity with a fused and elongated conjugated structure. One example belonging to this category is the pentacyclic thiophene-phenylene-thiophene **TPT** unit that has been successfully introduced to the D–A conjugated polymers and displays a promising photovoltaic performance (Scheme 1).[9]

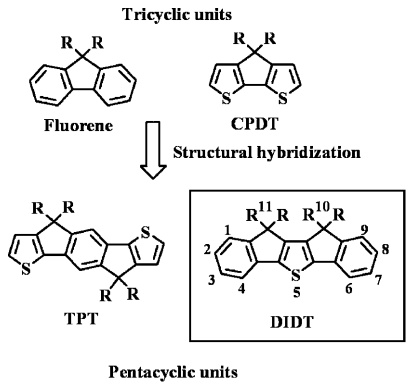

Scheme 1. Tricyclic structures of fluorene and **CPDT** units and their hybridized pentacyclic structures of **TPT** and **DIDT**.

On the other hand, diindeno[1,2-*b*:2′,1′-*d*]thiophene (**DIDT**)[10], another type of pentacyclic structure where the central thiophene is connected with two outer phenyl rings through two embedded CP rings, emerges as an appealing synthetic target, owing to its highly planar structure[11] (Scheme 1). To the best of our knowledge, however, this structure has never been incorporated into any conjugated polymer and thus its application in organic electronics has never been evaluated. We anticipate that this hybridized and expanded analogue may not only inherit the intrinsic advantages from its parent **CPDT** and fluorene units, but also lead to interesting electronic and optical properties attributable to a more planar conjugated structure.

Furthermore, the ability of functionalization at a bridging carbon allows for the introduction of four highly solubilizing aliphatic side chains without affecting its coplanarity, making **DIDT** derivatives highly soluble. Herein, for the first time, we report the detailed synthesis of the dibromo- and diboronic ester **DIDT** monomers. Accordingly, a series of donor–acceptor conjugated polymers consisting of **DIDT** units as a new electron-rich structure were successfully synthesized (Scheme 2). Their thermal, optical, and electrochemical properties have been carefully characterized. Preliminary tests of the photovoltaic performance based on these polymers show promise for solar cell applications.

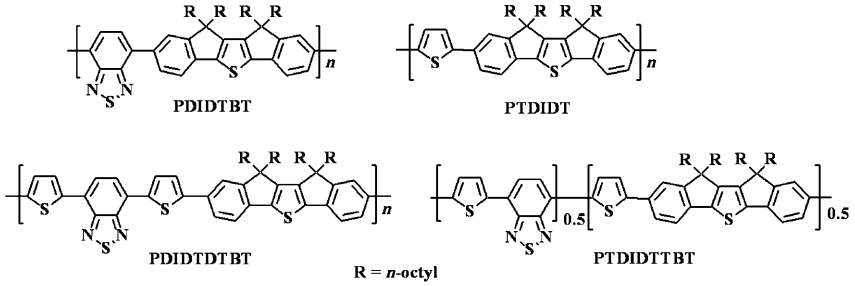

Scheme 2. The chemical structures of **PDIDTBT**, **PTDIDT**, **PDIDTDTBT**, and **PTDIDTTBT**.

Results and Discussion

Synthesis

The detailed synthesis of **DIDT** moieties is depicted in Scheme 3. Deprotonation of 1-indanone **1** by sodium hydride generated the corresponding enolate, which underwent oxidative dimerization in the presence of $CuCl_2$ to obtain compound **2** in 33% yield. Reaction of the 1,4-diketone in **2** with the commercially available Lawesson's reagent resulted in the formation of the central thiophene ring to afford compound **3** in 73% yield. The methylene protons at 10 and 11 positions in **3** are acidic enough to readily carry out alkylations in the presence of potassium hydroxide to yield **4** in 29% yield. Bromination of **4** by $Br_2/FeCl_3$ reagent regioselectively occurred at the 2, 8 positions to form compound **5** in a high yield of 83%. Upon treatment of **5** with *n*-butyl lithium followed by quenching with 2-isopropoxy-4,4,5,5-tet-

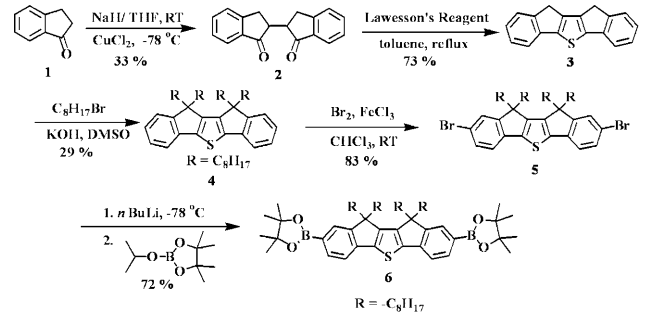

Scheme 3. Synthesis of **DIDT** monomer.

ramethyl-1,3,2-dioxaborolane, the boronic ester groups were successfully introduced to the 2, 8 positions to afford monomer **6** in 72% yield. With the donor monomers in hand, monomer **6** was polymerized with the acceptor units, 2,7-dibromo-benzothiadiazole **7** and 4,7-bis(5-bromothiophen-2-yl)2,1,3-benzothiadiazole **8**, by Suzuki cross-coupling to form alternating copolymer poly(diindenothiophene-*alt*-benzothiadiazole) **PDIDTBT** and poly(diindenothiophene-*alt*-dithienylbenzothiadiazole) **PDIDTDTBT**, respectively (Scheme 4). On the other hand, the copolymer

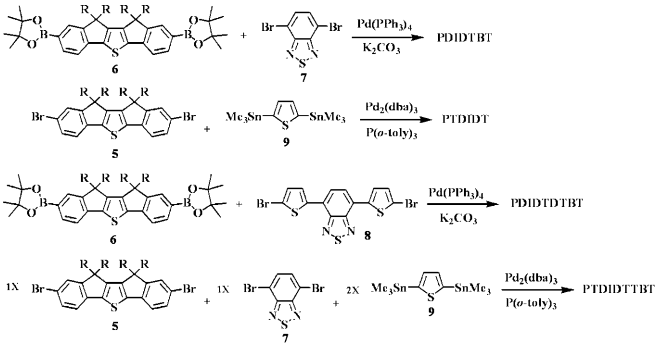

Scheme 4. Polymerization leading to **PDIDTBT**, **PTDIDT**, **PDIDTDTBT**, and **PTDIDTTBT**.

PTDIDTTBT was also prepared by reacting dibromo-monomers **5** and **7** with 2,5-bis(trimethylstannyl) thiophene **9** by Stille polymerization with the feed molar ratio of **5** to **7** to **9** being 1:1:2 (Scheme 4). After checking the ^{1}H NMR spectrum, we confirm that the final composition of the resulting **PTDIDTTBT** is consistent with original feed ratio of the monomers, meaning that the *m*/*n* ratio is approximately 0.5/0.5. In this manner, equal molar amounts of the **DIDT** donor and the benzothiadiazole acceptor are dispersed and separated by the unsubstituted thiophene spacers in the conjugated backbone. In terms of polymer composition, **PDIDTDTBT** and **PTDIDTTBT** actually have the same content of each component, which allows us to investigate the influence of monomer arrangement in the polymer chain on the intrinsic properties of copolymers. Finally, poly(thiophene-*alt*-diindenothiophene) **PTDIDT** was also prepared for structural comparison. All of the intermediates, monomers, and corresponding copolymers were fully characterized by using ^{1}H NMR and ^{13}C NMR spectroscopy (see the Supporting Information). The copolymers purified by successive re-precipitation and Soxhlet extraction showed narrow molecular weight distributions with a polydispersity index below two (Table 1). The number average molecular weight (M_n) of DIDT-based polymers is generally not high. This may arise from the fact that a DIDT-based pentacyclic monomer with large delocalized conjugated system may reduce its reactivity toward a cross-coupling reaction. All of the resulting copolymers showed excellent solubilities in common organic solvents, such as THF, chloroform, toluene, and 1,2-dichlorobenzene.

Table 1. Molecular weights, polydispersities, and thermal properties of polymers.

Copolymer	M_w[a]	M_n[a]	PDI[a]	T_g [°C]	T_m [°C]	T_d [°C][b]
PDIDTBT	7000	5000	1.40	58	–	398
PTDIDT	5000	4000	1.25	48	151	351
PDIDTDTBT	13000	7000	1.86	61	–	435
PTDIDTTBT	15000	11000	1.36	64	159	418

[a] Molecular weights and polydispersity were determined by gel permeation chromatography (GPC) in THF using polystyrene standards. [b] Decomposition temperature (5% weight loss) measured by TGA.

Thermal Properties and Polymer Arrangement

The thermal properties of **PTDIDTTBT**, **PDIDTBT**, and **PDIDTDTBT** were analyzed by using differential scanning calorimetry (DSC) and thermal gravimetric analysis (TGA) and the results are summarized in Table 1. The decomposition temperatures (T_d) of **PTDIDTTBT**, **PDIDTDTBT**, and **PDIDTBT** are 418, 435, and 398 °C, respectively (Figure 1), indicating their sufficient thermal stabilities for PSC applications. **PTDIDTTBT** and **PDIDTDTBT** copolymers, in which the repeating units have two additional thiophene rings in the main chain, are more thermally stable than **PDIDTBT**. Analysis of the DSC measurements reveals that

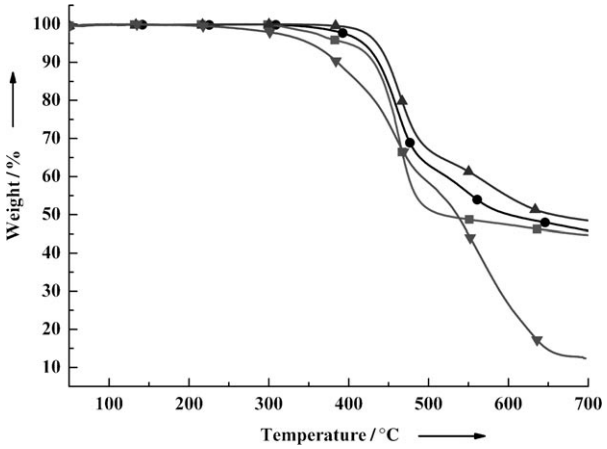

Figure 1. Thermal gravimetric analysis (TGA) measurements of **PDIDTBT** (■), **PDIDTDTBT** (▲), **PTDIDTTBT** (●), and **PTDIDT** (▼) with a ramping rate of 10 °C min^{-1}.

all of the polymers have a glass transition temperature of around 60 °C. However, it is rather surprising to observe that the alternating copolymer **PDIDTBT** and **PDIDTDTBT** did not show any transition of melting, whereas the random copolymer **PTDIDTTBT**, that supposedly possesses a more irregular structure, exhibited a melting point at 159 °C (Figure 2). This implies that

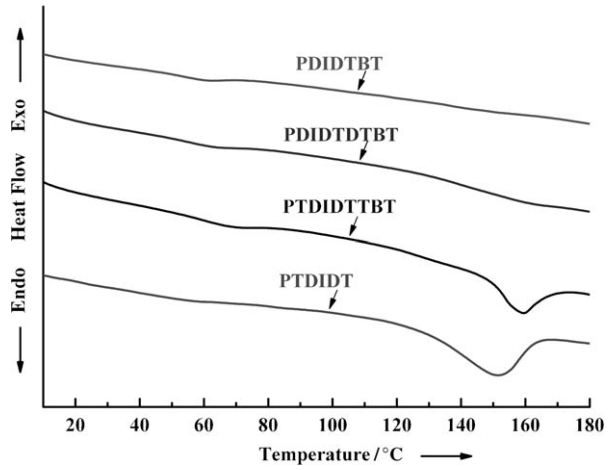

Figure 2. Differential scanning calorimeter (DSC) measurements of **PDIDTBT**, **PDIDTDTBT**, **PTDIDTTBT**, and **PTDIDT** with a ramping rate of 10 °C min^{-1}.

PTDIDTTBT is a semicrystalline copolymer that should possess a certain degree of structural regularity instead of random distribution at each component. We speculated that during the polymerization, the reactivities of two dibromo-monomers (**BT** and **DIDT**) toward the distannyl thiophene may vary considerably. Therefore, the 2,5-bis(trimethylstannyl) thiophene **9** may preferentially couple with the more reactive dibromo-monomer to form one block before reacting with the other less reactive monomer to form another block. To confirm this assumption, we monitored the progress of the polymerization by performing thin layer chromatography (TLC) and found that 2,7-dibromo-benzothiadiazole monomer **7** was consumed first, followed by the dibromo-**DIDT** monomer **5**. This finding is reasonable, considering that oxidative addition of a palladium complex into a carbon–bromine bond is facilitated if an electron-withdrawing substituent is introduced on the substrate.[12] In such an arrangement, the crystallinity of the **PTDIDTTBT** may arise from the block containing consecutive (thiophene-**DIDT**)$_n$ units, which are supposed to be more favorable to crystallize, owing to the rigid and planar structure of the **DIDT** unit. As a result, a truly alternating poly(thiophene-*alt*-diindenothiophene) **PTDIDT** was synthesized for comparison. The DSC measurement for the **PTDIDT** polymer exhibited a melting point at 151 °C, which is reminiscent of the behavior of **PTDIDTTBT**. ^{1}H NMR spectroscopy was employed to study the chemical environment of these polymers (Figure 3). The ^{1}H NMR spectra **PTDIDT** shows multiple peaks with an overlapped pattern in the region of $\delta =$

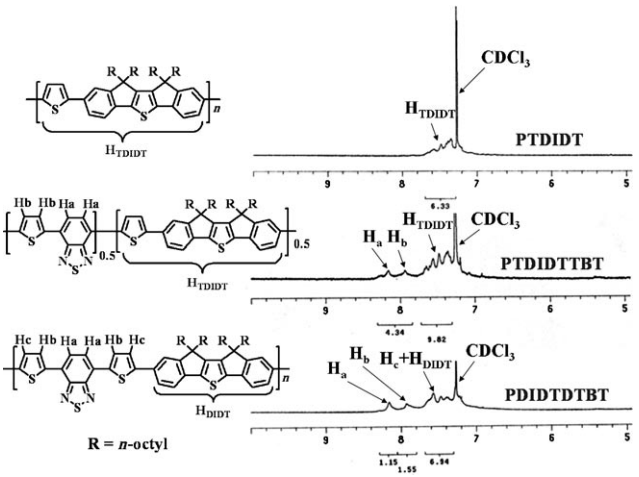

Figure 3. ^{1}H NMR spectra of **PTDIDT**, **PTDIDTTBT**, and **PDIDTDTBT** in the aromatic region ($CDCl_3$).

7.2–7.8 ppm undoubtedly owing to the protons (H_{TDIDT}) on the repeating (thiophene-**DIDT**)$_n$ units. Alternating **PDIDTDTBT** shows very different pattern of peaks in that region, whereas the pattern of peaks in **PTDIDTTBT** matches that of **PTDIDT** very well, which again proves that **PTDIDTTBT** indeed contains the (thiophene-**DIDT**)$_n$ block. Even though random polymerization using three monomers by means of Stille cross-coupling has been widely employed to tailor properties of polymers by varying the ratio of composition,[13] the coupling arrangement in the resulting polymer backbone has not been well studied. This is a very interesting finding in terms of making a new type of all conjugated block copolymer termed as (A-*alt*-B)$_n$-*b*-(A-*alt*-C)$_m$.

Optical and Electrochemical Properties

The absorption spectra of all studied polymers were measured in both dilute toluene (Figure 4) and in thin films (Figure 5), and the correlated optical parameters were summarized in Table 2.

All of the copolymers exhibit two distinct bands in the absorption spectra. One band in UV/Vis region is assigned to localized π–π^* transitions and the other band at longer wavelengths is attributed to intramolecular charge transfer (ICT) band between electron-rich donors and electron-deficient acceptors. By introducing thiophene units to the main chain to enhance the effective conjugation, both **PDIDTDTBT** and **PTDIDTTBT** exhibit significant red-shifted absorption spectra compared to **PDIDTBT**. Despite that alternating **PDIDTDTBT** and diblock **PTDIDTTBT** have the same three constituents (thiophene, **BT**, and **DIDT**), the arrangement of their relative positions in the polymeric backbone significantly affects the optical properties. The intensity of the ICT band is slightly stronger than that of the π–π^* transition band of the alternating **PDIDTDTBT** in the thin film. On the contrary, the π–π^* transition absorption band is much larger than the ICT band

CHEMISTRY
AN ASIAN JOURNAL

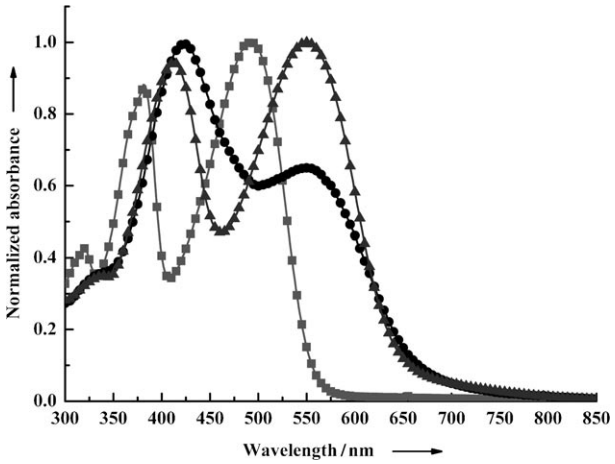

Figure 4. Normalized absorption spectra of **PDIDTBT** (■), **PDIDTDTBT** (▲), and **PTDIDTTBT** (●) in toluene solution.

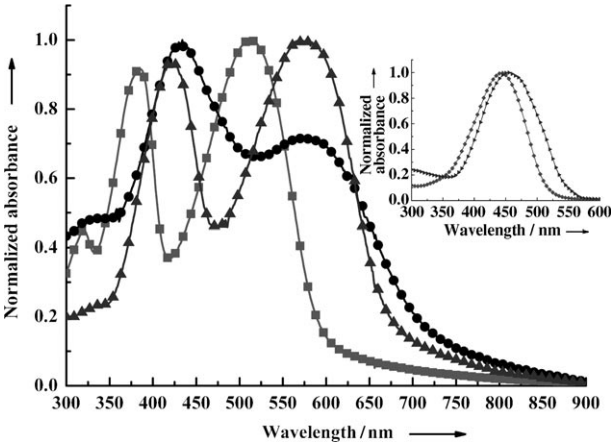

Figure 5. Normalized absorption spectra of **PDIDTBT** (■), **PDIDTDTBT** (▲), and **PTDIDTTBT** (●) in the thin film. The absorption spectra of **PTDIDT** in toluene solution (◆) and in the thin film (▶) are also shown in the inset.

Table 2. Optical properties and band gaps of the copolymers in the toluene solution and in the thin film.

Polymer	Toluene solution		Thin film		
	λ_{max} [nm]	λ_{onset} [nm]	λ_{max} [nm]	λ_{onset} [nm]	E_g^{opt} [eV]
PDIDTBT	381, 491	559	385, 512	594	2.09
PTDIDT	443	521	454	560	2.21
PDIDTDTBT	412, 550	649	425, 569	671	1.85
PTDIDTTBT	423, 549	661	434, 573	717	1.73

in the diblock **PTDIDTTBT**. For comparison, we measured the absorption spectrum of the reference copolymer **PTDIDT**, which showed a single band located in the range $\lambda = 350$–550 nm. This result confirms that the higher energy π–π^* transition bands in **PDIDTDTBT** and **PTDIDTTBT** are originated from the -(thiophene-**DIDT**)$_n$- units. The more repeating units of thiophene-**DIDT** connect together, the more intense and red-shifted the absorption band can be observed in this region. Consequently, the stronger intensity of the π–π^* transition band in **PTDIDTTBT** reasonably supports the speculation that this polymer contains a block with a repeating thiophene-**DIDT** unit. Although the profiles of the absorption spectra of the three polymers are essentially unchanged, all of the spectra shift toward longer wavelengths from solution to the solid state, indicating that the planar structure of **DIDT** is capable of inducing strong interchain π–π interactions. The optical bandgaps (E_g^{opt}) deduced from the absorption edges of thin film spectra are in the following order: **PTDIDTTBT** (1.73 eV) < **PDIDTDTBT** (1.85 eV) < **PDIDTBT** (2.09 eV). Compared with alternating **PDIDTDTBT**, diblock **PTDIDTTBT** has a smaller optical bandgap mainly as a result of its stronger intermolecular interactions in the solid state, which is also correlated to the higher tendency of **PTDIDTTBT** toward crystallization. Fluorescence properties of these polymers in dilute solution were also investigated (Figure 6). Excitation of **PTDIDT** at

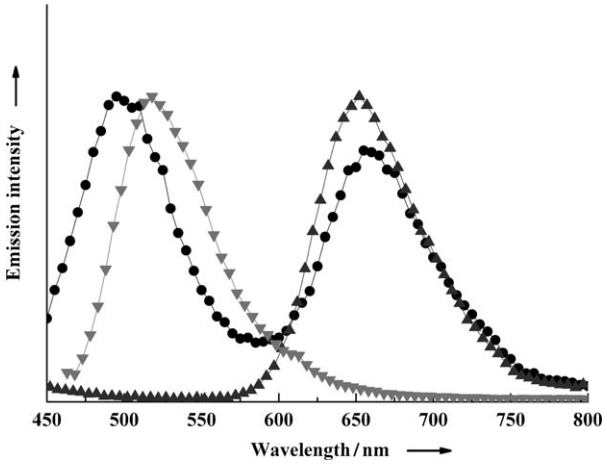

Figure 6. Normalized fluorescence spectra of **PDIDTDTBT** (▲; λ_{ex} = 412 nm), and **PTDIDTTBT** (●; λ_{ex} = 423 nm), and **PTDIDT** (▼; λ_{ex} = 443 nm) in the dilute toluene solution.

$\lambda = 443$ nm produced a clear emission band at $\lambda = 520$ nm clearly resulting from the -(thiophene-**DIDT**)$_n$- moieties. When the **PDIDTDTBT** solution was excited at $\lambda = 412$ nm, which is the absorption λ_{max} of the donor segment, the emission from the donor segment was completely quenched and only the fluorescence from the acceptor at $\lambda = 660$ nm was observed. These results suggest that intrachain energy transfer from the electron-rich thiophene-**DIDT** to the electron-deficient benzothiadiazole moieties occurs efficiently, owing to the close proximity between the donor and acceptor units along the polymer chain. In contrast, upon excitation of **PTDIDTTBT** at $\lambda = 423$ nm, in addition to the emission from the acceptor part, the donor emission with significant intensity was also observed, indicative of the relatively poor efficiency of energy transfer. This result again strongly implies that **PTDIDTTBT** has a diblock arrangement, so that energy transfer can only occur near the junctions of the two blocks.

Cyclic voltammetry (CV) was employed to examine the electrochemical properties and evaluate the HOMO and LUMO levels of the polymers (Table 3 and Figure 7). All of the polymers showed stable and reversible p-doping and n-doping processes, which are important prerequisites for p-type semiconductor materials. HOMO energy level of a D–A conjugated polymer is generally determined by its electron-rich segment. The HOMO energy level of **PDIDTBT** is estimated to be −5.51 eV, which indicates that **DIDT** is a good electron-rich unit to construct a polymer with a low-lying HOMO level. The incorporation of the thiophene units into the main chains of **PTDIDTTBT** and **PDIDTDTBT**, raises up the HOMO levels to −5.35 and −5.36 eV, respectively. According to the HOMO–LUMO energy difference, the electrochemical bandgaps E_g^{el} were also calculated to be 2.03, 2.13, and 2.44 eV for **PTDIDTTBT**, **PDIDTDTBT**, and **PDIDTBT**, respectively. The E_g^{el} values are slightly greater than E_g^{opt}, a phenomenon consistent with the reports in the literature.[14] An energy diagram of HOMO–LUMO levels of **PDIDTBT**, **PDIDTDTBT**, and **PTDIDTTBT** relative to $PC_{71}BM$ are shown in Figure 8.

Table 3. Electrochemical onset potentials and electronic energy levels of the polymers.

Copolymer	E_{ox}^{onset} [V]	E_{red}^{onset} [V]	HOMO [eV]	LUMO^{el} [eV]	LUMO$^{opt[a]}$ [eV]	E_g^{el} [eV]
PDIDTBT	0.71	−1.73	−5.51	−3.07	−3.42	2.44
PDIDTDTBT	0.56	−1.57	−5.36	−3.23	−3.51	2.13
PTDIDTTBT	0.55	−1.48	−5.35	−3.32	−3.62	2.03

[a] LUMO levels of the polymers were obtained from the equation LUMO = HOMO + E_g^{opt}.

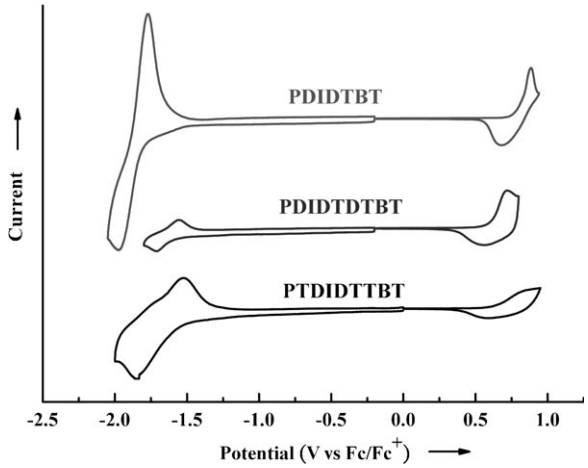

Figure 7. Cyclic voltammograms of **PDIDTBT**, **PDIDTDTBT**, and **PTDIDTTBT** films on glassy carbon electrode at a scan rate of 80 mV s^{-1}.

Hole-mobility and Photovoltaic Characteristics

Hole-only devices (ITO/PEDOT:PSS/polymer/Au) were fabricated to estimate the hole mobilities of these polymers by means of the space-charge limit current (SCLC) theory. Bulk heterojunction photovoltaic cells were also fabricated on the basis of ITO/PEDOT:PSS/polymer:$PC_{71}BM$/Ca/Al configuration and their performances were measured under 100 mW cm^{-2} AM 1.5 illumination. $PC_{71}BM$ was used, owing to its stronger light absorption in the visible region than that of $PC_{61}BM$.[15] The characterization data are summarized in Table 4 and the *J–V* curves of these polymers are shown in Figure 9. The device based on **PDIDTBT**/$PC_{71}BM$ (1:1, w/w) blend exhibited a V_{oc} of 0.70 V, a J_{sc} of 3.3 mA cm^{-2}, and a fill factor (FF) of 33%, producing a PCE of 0.76%. This relatively lower performance can be ascribed to the poorer absorption ability and lower hole-mobility (3×10^{-5} cm^2 V s) of **PDIDTBT**. On the other hand, the **PDIDTDTBT**/$PC_{71}BM$ (1:2, w/w) based device showed a better J_{sc} of 5.3 mA cm^{-2} and FF of 44%, improving the PCE to 1.65%. Finally, the **PTDIDTTBT**/$PC_{71}BM$ (1:4, w/w) based device exhibited the best performance with a highest J_{sc} of 6.2 mA cm^{-2} and a PCE of 2.00%. The broader absorption spectrum of **PTDIDTTBT** might be responsible for its better photocurrent and performance over the **PDIDTDTBT**-based device.

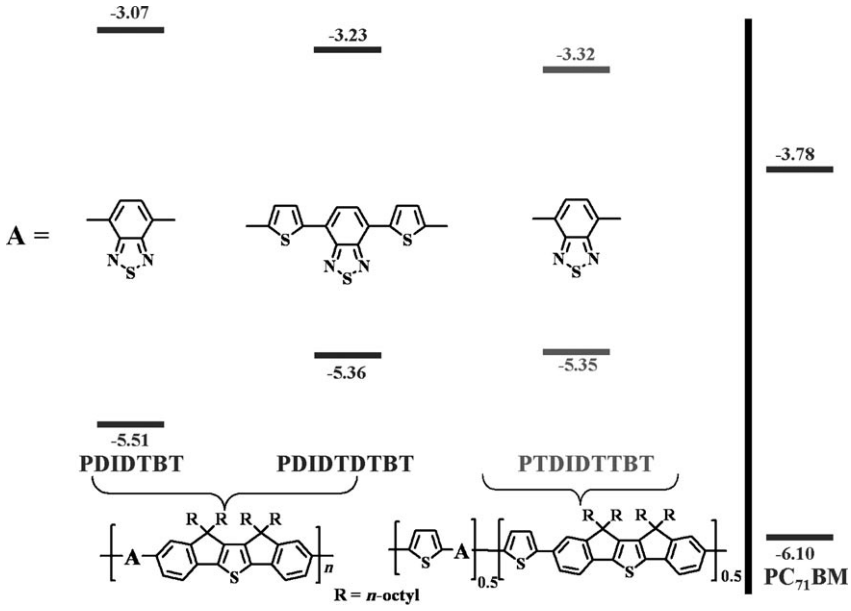

Figure 8. Energy diagram of HOMO–LUMO levels for **PDIDTBT**, **PDIDTDTBT**, **PTDIDTTBT**, and $PC_{71}BM$.

Table 4. Photovoltaic characteristics.

Copolymer	The wt% ratio of Copolymer and $PC_{71}BM$	Mobility [$cm^2V^{-1}s$]	V_{oc} [V]	J_{sc} [$mA\,cm^{-2}$]	FF [%]	PCE [%]
PDIDTBT	1:1	3×10^{-5}	0.70	3.3	33	0.76
PDIDTDTBT	1:2	1×10^{-4}	0.70	5.3	44	1.65
PTDIDTTBT	1:4	3×10^{-5}	0.68	6.2	47	2.00
PTDIDTTBT/ PDIDTDTBT	1:1:8	–	0.85	6.4	43	2.40

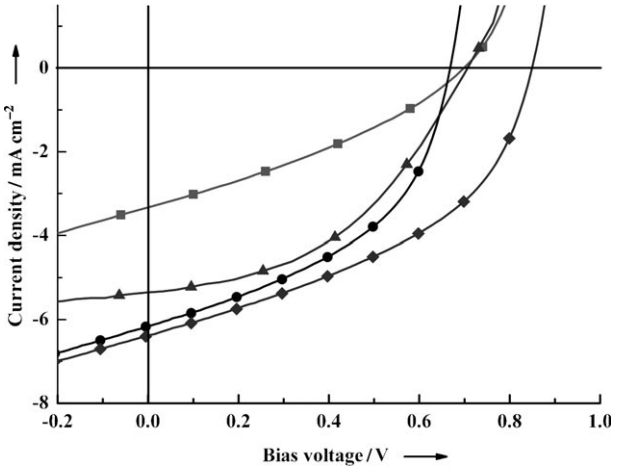

Figure 9. *J–V* characteristics of ITO/PEDOT:PSS/polymer:$PC_{71}BM$/Ca/Al under illumination of AM1.5, 100 $mW\,cm^{-2}$. **PDIDTBT** (■), **PDIDTDTBT** (▲), **PTDIDTTBT** (●), and **PDIDTDTBT**+**PTDIDTTBT** (◆).

Although **PTDIDTTBT** and **PDIDTDTBT** represent the best of two **DIDT**-based polymers in this study, further improvement of these materials to achieve higher device performance is desirable. Very recently, we have demonstrated that performance of PSCs can be improved by using a ternary blend in an active layer.[16] In addition to a typical n-type PCBM-based material, this ternary blend should contain two p-type polymers, which have complementary absorption spectra and are structurally compatible. Compared with the optical properties of **PDIDTDTBT**, **PTDIDTTBT** has a weaker ICT band, but a stronger and broader π–π^* transition band. It is envisaged that the combination of **PTDIDTTBT** and **PDIDTDTBT** may strengthen the absorption ability to harvest sunlight more effectively. Note that the HOMO values of the two donor polymers **PTDIDTTBT** and **PDIDTDTBT** (−5.36 eV and −5.35 eV, respectively) are also close to each other. A BHJ device with an active layer containing the ternary blend of **PDIDTDTBT**/**PTDIDTTBT**/$PC_{71}BM$ (1:1:8 in wt%) was consequently fabricated and investigated. Based on the **PTDIDTTBT**/$PC_{71}BM$ binary blend in which the optimal blending ratio of p-type to n-type materials is 1:4 (wt%), the composition of the ternary blend of **PDIDTDTBT**/**PTDIDTTBT**/$PC_{71}BM$ was determined to be 1:1:8 (wt%). This device showed the best performance, reaching a V_{oc} of 0.85 V, a J_{sc} of 6.4 $mA\,cm^{-2}$, a FF of 43%, and a PCE of 2.40%. The device based on the ternary blend outperforms the devices based on the binary systems, **PDIDTDTBT**/$PC_{71}BM$ or **PTDIDTTBT**/$PC_{71}BM$.

The morphology of the active layer blends in the devices play an important role in determining the device performance and was thus investigated using tapping-mode atomic force microscopy (AFM).[17] Each sample was prepared using identical conditions for the fabrication of the devices. The topography and phase images are shown in Figure 10. The **PDIDTDTBT**/$PC_{71}BM$ (1:2, w/w) blend showed more homogeneous mixing without obvious phase separation, whereas localized nanofibers were observed in the **PTDIDTTBT**/$PC_{71}BM$ (1:4, w/w) blend. This result correlates highly with the amorphous and semicrystalline nature for the alternating **PDIDTDTBT** and diblock **PTDIDTTBT**, respectively. By combining **PDIDTDTBT** with **PTDIDTTBT** together, the ternary **PDIDTDTBT**/**PTDIDTTBT**/$PC_{71}BM$ (1:1:8, w/w/w) blend exhibited a smoother surface film with nanoscale phase separation. We conclude that the improved V_{oc} and J_{sc} of the ternary system might arise from the better morphology to facilitate charge transport and better absorption to match the solar spectrum.

Conclusions

We have successfully synthesized the pentacyclic diindeno[1,2-*b*:2′,1′-*d*]thiophene (**DIDT**) tetra-alkylated **DIDT** molecule, as well as its 2,8-dibromo- and 2,8-diboronic ester derivatives, which are readily polymerized into various donor–acceptor **DIDT**-based conjugated polymers. Two alternating poly(diindenothiophene-*alt*-benzothiadiazole) **PDIDTBT** and poly(diindenothiophene-*alt*-dithienylbenzothiadiazole) **PDIDTDTBT** were synthesized by Suzuki polymerization. **PTDIDTTBT** was also prepared by reacting the dibromo-**DIDT 5** and 2,7-dibromo-benzothiadiazole **7** with 2,5-bis(trimethylstannyl) thiophene **9** by Stille polymerization. Interestingly, despite that **PTDIDTTBT** is prepared in a manner of random polymerization, it was found that the different reactivities of the monomers led to the resulting polymer having an arrangement of a block copolymer. The higher structural regularity of **PTDIDTTBT**, symbolized as (thiophene-*alt*-**DIDT**)$_{0.5}$-*block*-(thiophene-*alt*-BT)$_{0.5}$, leads to many interesting properties, including the stronger π–π stacking, tendency of crystallization, and broader absorption spectrum. All-conjugated rod–rod block copolymers have come into the focus of interest recently because of their unique optical and electronic properties, as well as their abilities to form self-assembled nanostructures.[18] However, the amount of research is rather limited mainly owing to the synthetic challenge. We have demonstrated that by differentiating the reactivities of monomers in the metal-catalyzed polycondensation, an all-conjugated rod–

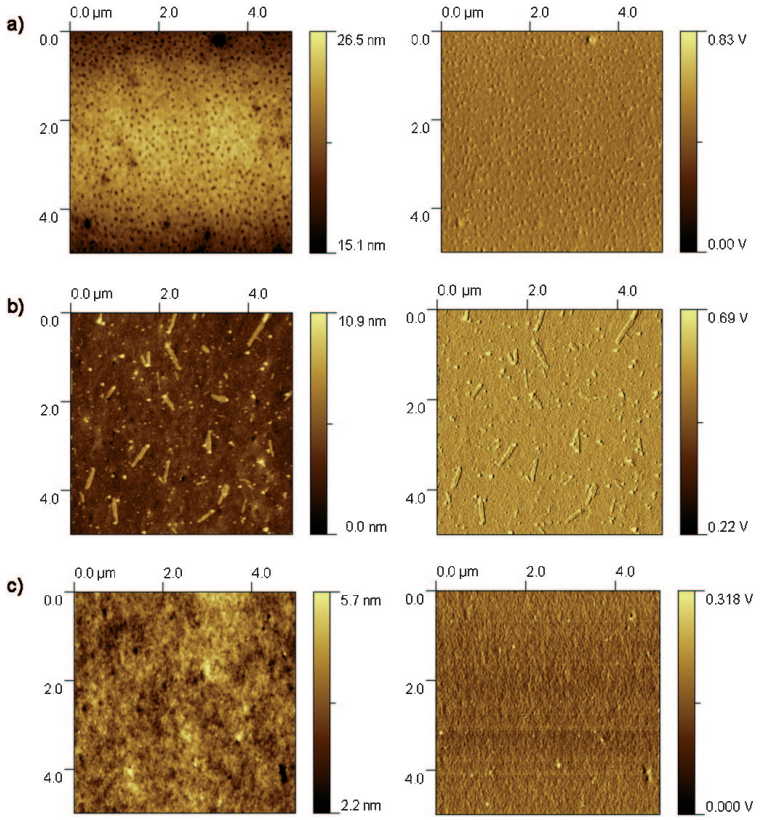

Figure 10. a) AFM images of the **PDIDTDTBT**/$PC_{71}BM$ blend, b) **PTDIDTTBT**/PCBM blend and c) **PDIDTDTBT**/**PTDIDTTBT**/$PC_{71}BM$ blend. The topography of each film is shown in the left, and the corresponding phase image in the right.

rod block copolymer termed as (A-*alt*-B)$_n$-*block*-(A-*alt*-C)$_m$ can be easily realized. Optical, electrical, and morphological properties of the conjugated polymers can be thus tailored through controlling the arrangement of each monomeric component. Bulk heterojunction photovoltaic cells based on ITO/PEDOT:PSS/polymer:$PC_{71}BM$/Ca/Al configuration were fabricated and characterized. **PDIDTDTBT**/$PC_{71}BM$ and **PTDIDTTBT**/$PC_{71}BM$ systems exhibited promising PCEs of 1.65 and 2.00%, respectively. The PCE of the device based on a ternary blend **PDIDTDTBT**/**PTDIDTTBT**/$PC_{71}BM$ was further improved to 2.40%.

Experimental Section

General Measurement and Characterization

All chemicals are purchased from Aldrich or Acros and used as received unless otherwise specified. ^1H and ^{13}C NMR spectroscopy experiments were completed by using a Varian 300 MHz spectrometer. The molecular weight of polymers was measured by using GPC (Viscotek VE2001GPC), and polystyrene was used as the standard (THF as the eluent). The differential scanning calorimetry used was a TA Q200 calorimeter and the thermal gravimetric analysis was recorded by using a Perkin–Elmer Pyris under a nitrogen atmosphere at a heating rate of 10 °C min^{-1}. Absorption spectra were taken by using a HP8453 UV/Vis spectrophotometer. Photoluminescence (PL) emission spectra were measured in the dilute toluene solution (10^{-5}–10^{-6} M) on an ARC SpectraPro-150 spectrofluorimeter. The electrochemical cyclic voltammetry was conducted by using a Bioanalytical Systems Inc. analyzer. A glassy carbon electrode coated with a thin polymer film was used as the working electrode, an Ag/AgCl electrode as the reference, and 0.1 M tetrabutylammonium hexafluorophosphate ($TBAPF_6$) in acetonitrile was the electrolyte. Cyclic voltammetry curves were calibrated by using ferrocence, as the standard, for which the HOMO is set at −4.8 eV with respect to zero vacuum level. The HOMO energy levels were obtained from the equation HOMO = −e ($E_{ox}^{onset} - E_{(ferrocene)}^{onset} + 4.8$) eV. The LUMO levels of polymer were obtained from the equation LUMO = −e ($E_{red}^{onset} - E_{(ferrocene)}^{onset} + 4.8$) eV.

Fabrication and Characterization of BHJ Devices

The ITO/glass substrates were ultrasonically cleaned sequentially in detergent, water, acetone, and isopropyl alcohol. Then, the substrates were covered by a 30 nm thick layer of PEDOT:PSS (Clevios P provided by H. C. Stark) by spin coating. After annealing in air at 200 °C during 10 min, the samples were cooled down to room temperature (RT). Polymers were dissolved in *ortho*-dichlorobenzene (ODCB) (0.5–1.0 wt.%) and $PC_{71}BM$ (purchased from Nano-C) was added to reach the desired ratio. The solution was then heated at 70 °C over 1 hour and stirred overnight at RT. Prior to deposition, the solution was filtrated through a 0.45 μm filter and the substrates were transferred in a glove box. The photoactive layer was then coated at different spin-coating speeds to tune its thickness. After drying, the samples were annealed for 15 min. The detailed processing parameters (spin coating speed; annealing temperature) are shown as follows: **PDIDTBT**/$PC_{71}BM$ (1400 rpm; 140 °C), **PDIDTDTBT**/$PC_{71}BM$ (1400 rpm, without annealing), **PTDIDTTBT**/$PC_{71}BM$ (1500 rpm; 110 °C), **PDIDTDTBT**/**PTDIDTTBT**/$PC_{71}BM$ (1500 rpm; 110 °C). The cathode made of calcium (35 nm thick) and aluminum (100 nm thick) was evaporated through a shadow mask under high vacuum ($<10^{-6}$ torr). Each device is constituted of 4 pixels defined by an active area of 0.04 cm^2. Finally, the devices were encapsulated and *I–V* curves were measured in air.

Electrical Characterization under Illumination

The devices were characterized by using 100 mW cm^{-2} AM 1.5 simulated light measurement (Yamashita Denso solar simulator). Current-voltage (*J–V*) characteristics of PSC devices were obtained by using a Keithley 2400 SMU. Solar illumination conforming to the JIS Class AAA was provided by a SAN-EI 300W solar simulator equipped with an AM 1.5G filter. The light intensity was calibrated by using a Hamamatsu S1336–5BK silicon photodiode. The performances presented here are the average of the 4 pixels of each device.

Hole-only Devices

To investigate the respective hole mobility of the different copolymer films, unipolar devices have been prepared following the same procedure except that the active layer is made of pure polymer and the Ca/Al cathode is replaced by evaporated gold (40 nm). The hole mobilities were calculated according to space charge limited current theory (SCLC). The *J–V* curves were fitted according to the following Equation (1):

$$J = \frac{9}{8}\varepsilon\mu\frac{V^2}{L^3} \quad (1)$$

for which ε is the dielectric permittivity of the polymer, μ is the hole mobility and L is the film thickness (distance between the two electrodes).

*Synthesis of 2,2′-Biindanyl-1,1′-dione (**2**)*[10a]

To a suspension of sodium hydride (1.65 g, 41.6 mmol; 60% oil dispersion) in dry THF (75 mL) under nitrogen was added a THF solution (125 mL) of 1-indanone **1** (5 g, 38 mmol) dropwise at RT. The resulting mixture was stirred at RT until there was no further evolution of hydrogen gas. The reaction mixture was cooled to −78 °C, and copper chloride (5.64 g, 41.6 mmol) was added in one portion. After stirring at −78 °C for 30 min, the suspension was warmed up to RT and after stirring for another 30 min, the mixture was quenched with water (50 mL). The THF was removed under reduced pressure, the reaction solution was extracted with ether (300 mL×3) and water (150 mL). The combined organic layer was dried over $MgSO_4$. After removal of the solvent under reduced pressure, the residue was purified by column chromatography on silica gel (hexane/ethyl acetate, v/v, 5/1) to give a brown solid **2** (1.64 g, 33%), (*meso*/*d*,*l* mixture); m.p.: 142–143 °C; ^{1}H NMR ($CDCl_3$, 300 MHz): δ = 2.49 (dd, J_1 = 3.9, J_2 = 17.4 Hz, 1H), 3.01 (dd, J_1 = 3.9, J_2 = 17.4 Hz, 1H), 3.17–3.58 (m, 4H), 7.36–7.47 (m, 4H), 7.59 (t, J = 5.1 Hz, 2H), 7.79 ppm (t, J = 9.0 Hz, 2H); ^{13}C NMR ($CDCl_3$, 75 MHz): δ = 28.2, 30.7, 47.0, 48.2, 123.9, 124.0, 126.5, 126.6, 127.5, 127.6, 134.8, 135.1, 136.8, 136.9, 153.3, 153.7, 206.2, 207.4 ppm; MS (EI) calcd for $C_{18}H_{14}O_2$: 262.30; found: 262.

*Synthesis of 10,11-Dihydrodiindeno[1,2-b:2′1′-d]thiophene (**3**)*

To a solution of **2** (1.64 g, 6.25 mmol) in dry toluene (56 mL) under nitrogen was added Lawesson's reagent [2,4-bis(4-methoxyphenyl)-1,3-dithia-2,4-diphosphetane 2,4-disulfide] (3.03 g, 7.50 mmol) in one portion. The resulting mixture was heated at reflux for 2.5 h. Toluene was removed under reduced pressure and the residue was recrystallized from chloroform to give a pale cream-colored crystal **3** (1.19 g, 73%); m.p.: 290 °C; ^{1}H NMR ($CDCl_3$, 300 MHz): δ = 3.72 (s, 4H), 7.19 (t, J = 7.5 Hz, 2H), 7.33 (t, J = 7.95 Hz, 2H), 7.49 ppm (d, J = 7.8 Hz, 4H); ^{13}C NMR ($CDCl_3$, 75 MHz): δ = 33.3, 118.4, 124.6, 125.1, 127.0, 139.6, 141.6, 145.4, 145.7 ppm; MS (EI) calcd for $C_{18}H_{12}S$: 260.35; found: 260.

*10,10,11,11-Tetraoctyl-diindeno[1,2-b:2′1′-d]thiophene (**4**)*

To a suspension solution of **3** (2.70 g, 10 mmol), octyl bromide (16.02 g, 83 mmol) and potassium iodide (40 mg) in DMSO (270 mL) was added potassium hydroxide (5.4 g, 96.2 mmol) in one portion at 0 °C. The resulting solution was stirred for 16 h at 80 °C and then was extracted with ether (350 mL×3) and water (150 mL). The combined organic layer was dried over $MgSO_4$. After removal of the solvent under reduced pressure, the residue was purified by column chromatography on silica gel (hexane) to give a yellow solid **4** (2.11 g, 29%); m.p.: 153 °C ^{1}H NMR ($CDCl_3$, 300 MHz): δ = 0.59–1.45 (m, 60H), 2.06 (t, J = 8.1 Hz, 8H), 7.11–7.29 (m, 6H), 7.35 ppm (d, J = 7.2 Hz, 2H); ^{13}C NMR ($CDCl_3$, 75 MHz): δ = 14.0, 22.6, 24.1, 29.5, 29.6, 30.3, 31.9, 40.3, 55.3, 117.8, 121.9, 124.9, 126.7, 139.1, 144.5, 148.9, 152.3 ppm; MS (EI) calcd for $C_{50}H_{76}S$: 709.20; found: 709.

*2,8-Dibromo-10,10,11,11-tetraoctyl-diindeno[1,2-b:2′1′-d]thiophene (**5**)*

To a solution of **4** (1.51 g, 2.13 mmol) and iron(III) chloride (45 mg) in chloroform (30 mL) was added bromine (0.71 g, 4.47 mmol) in chloroform (18 mL) dropwise at room temperature. The resulting solution was stirred for 12 h at RT and then was quenched by saturated sodium thiosulfate solution (100 mL). The mixture solution was extracted with chloroform (250 mL×3) and water (100 mL). The combined organic layer was dried over $MgSO_4$. After removal of the solvent under reduced pressure, the residue was purified by column chromatography on silica gel (hexane) to give a pale-yellow solid **5** (1.53 g, 83%); m.p.: 116 °C; ^{1}H NMR ($CDCl_3$, 300 MHz): δ = 0.57–1.40 (m, 60H), 1.95–2.15 (m, 8H), 7.21 (d, J = 8.0 Hz, 2H), 7.33 (d, J = 1.7 Hz, 2H), 7.38 ppm (dd, J_1 = 1.7, J_2 = 8.0 Hz, 2H); ^{13}C NMR ($CDCl_3$, 75 MHz): δ = 14.0, 22.6, 24.1, 29.4, 29.6, 30.2, 31.8, 40.2, 55.8, 119.0, 119.2, 125.2, 130.0, 137.8, 144.1, 149.0, 154.5 ppm; MS (EI) calcd for $C_{50}H_{74}Br_2S$: 867.0; found: 867; elemental analysis (%) calcd for $C_{50}H_{74}Br_2S$: C 69.27, H 8.60; found: C 69.35, H 8.61.

*2,8-bis(4,4,5,5,-tetramethyl-1,3,2-dioxaborolan-2-yl)-10,10,11,11-tetraoctyl-diindeno[1,2-b:2′1′-d]thiophene (**6**)*

To a solution of **5** (1.06 g, 1.22 mmol) in dry THF (28 mL) was added 2.5 M solution of *n*BuLi (1.6 mL in hexane, 3.91 mmol) dropwise at −78 °C. The resulting mixture was stirred for 2 h at −78 °C. 2-Isopropoxy-4,4,5,5-tetramethyl-1,3,2-dioxaborolane (0.91 g, 4.89 mmol) was added to the mixture solution dropwise. The mixture was allowed to warm up to RT and then stirred for 16 h. Water (150 mL) was added to the reaction which was then extracted wth ethyl acetate (300 mL×3). The combined organic layer was dried over $MgSO_4$. After removal of the solvent under reduced pressure, the residue was purified by column chromatography on silica gel (hexane/ethyl acetate, v/v, 40/1) and then recrystallized from methanol to give a yellow solid **6** (0.85 g, 72%); m.p.: 171 °C; ^{1}H NMR ($CDCl_3$, 300 MHz): δ = 0.50–1.30 (m, 60H), 1.39 (s, 12H), 1.98–2.18 (m, 8H), 7.37 (d, J = 7.4 Hz, 2H), 7.60 (s, 2H), 7.74 ppm (d, J = 7.4 Hz, 2H); ^{13}C NMR ($CDCl_3$, 75 MHz): δ = 14.0, 22.6, 24.0, 24.9, 29.5, 29.6, 30.2, 31.8, 40.1, 55.5, 83.6, 117.3, 127.6, 134.0, 141.9, 145.3, 150.2, 151.5 ppm; MS (EI) calcd for $C_{62}H_{98}B_2O_4S$: 961.13; found: 961; elemental analysis (%) calcd for $C_{62}H_{98}B_2O_4S$: C 77.48, H 10.28; found: C 77.81, H 9.65.

Synthesis of PTDIDTTBT

To a 100 mL round bottom flask was introduced **5** (634 mg, 0.73 mmol), 4,7-dibromo-2,1,3-benzothiadiazole **7** (215 mg, 0.73 mmol), 2,5-bis(trimethylstannyl) thiophene **9** (600 mg, 1.46 mmol), [$Pd_2(dba)_3$] (53.6 mg, 0.059 mmol), tri(*o*-tolyl)phosphine (142.6 mg, 0.47 mmol) and chlorobenzene (50 mL). The mixture was then degassed by bubbling nitrogen for 10 min at RT. The round bottom flask was placed into the microwave reactor and reacted for 45 min under 270 Watt. The solution was added into methanol dropwise. The precipitate was collected by filtration and washed by Soxhlet extraction with acetone, ethyl acetate, and THF, sequentially for one week. The Pd-thiol gel (Silicycle Inc.) was added to above THF solution to remove the residual Pd catalyst. After filtration and removal of the solvent, the polymer was re-dissolved in THF again and added into methanol to re-precipitate out. The purified polymer was collected by filtration and dried under vacuum for 1 day to give a dark solid (170 mg, 23%, M_n = 11000, PDI = 1.36). ^{1}H NMR ($CDCl_3$, 300 MHz): δ = 0.50–1.40 (m, 60H), 1.95–2.15 (m, 8H), 7.20–7.70 (m, 8H), 7.90–8.30 ppm (m, 4H).

Synthesis of PTDIDT

To a 100 mL round bottom flask was introduced **5** (200 mg, 0.23 mmol), 2,5-bis(trimethylstannyl) thiophene **9** (95 mg, 0.23 mmol), [$Pd_2(dba)_3$] (8.5 mg, 0.0092 mmol), tri(*o*-tolyl)phosphine (22.5 mg, 0.074 mmol), and chlorobenzene (8 mL). The mixture was then degassed by bubbling nitrogen for 10 min at RT. The round bottom flask was placed into the microwave reactor and reacted for 45 min under 270 Watt. The solution was added into methanol dropwise. The precipitate was collected by filtration and washed by Soxhlet extraction with acetone, ethyl acetate, and THF sequentially for one week. The Pd-thiol gel (Silicycle Inc.) was added to above THF solution to remove the residual Pd catalyst. After filtration and removal of the solvent, the polymer was re-dissolved in THF again and added into methanol to re-precipitate out. The purified polymer was collected by filtration and dried under vacuum for 1 day to give a brown solid (51 mg, 28%, M_n = 4000, PDI = 1.25). ^{1}H NMR ($CDCl_3$, 300 MHz): δ = 0.50–1.40 (m, 60H), 2.00–2.20 (m, 8H), 7.30–7.70 ppm (m, 8H).

Synthesis of PDIDTBT

To a 50 mL round bottom flask was introduced **6** (300 mg, 0.31 mmol), 4,7-dibromo-2,1,3-benzothiadiazole **7** (92 mg, 0.31 mmol), [$Pd(PPh_3)_4$] (7.2 mg, 0.0063 mmol), K_2CO_3 (330 mg, 2.36 mmol), degas toluene (10 mL), and degas H_2O (2 mL). The mixture was heated to 110 °C under nitrogen gas for 72 h. The solution was added into methanol dropwise. The precipitate was collected by filtration and washed by Soxhlet extraction with methanol, acetone, and THF sequentially for one week. The

Pd-thiol gel (Silicycle Inc.) was added to above THF solution to remove the residual Pd catalyst. After filtration and removal of the solvent, the polymer was re-dissolved in THF again and added into methanol to re-precipitate out. The purified polymer was collected by filtration and dried under vacuum for 1 day to give a dark solid (130 mg, 50%, M_n = 5000, PDI = 1.40). ^{1}H NMR ($CDCl_3$, 300 MHz): δ = 0.50–1.30 (m, 60H), 1.90–2.35 (m, 8H), 7.50–7.70 (m, 2H), 7.80–8.10 ppm (m, 6H).

Synthesis of PDIDTDTBT

To a 50 mL round bottom flask was introduced **6** (300 mg, 0.31 mmol), 4,7-bis(5-bromothiophen-2-yl)2,1,3-benzothiadiazole **8** (139 mg, 0.31 mmol), [$Pd(PPh_3)_4$] (7.2 mg, 0.0063 mmol), K_2CO_3 (330 mg, 2.36 mmol), degas toluene (10 mL), and degas H_2O (2 mL). The mixture was heated to 110 °C under nitrogen gas for 72 h. The solution was added into methanol dropwise. The precipitate was collected by filtration and washed by Soxhlet extraction with methanol, acetone, and THF sequentially for one week. The Pd-thiol gel (Silicycle Inc.) was added to above THF solution to remove the residual Pd catalyst. After filtration and removal of the solvent, the polymer was re-dissolved in THF again and added into methanol to re-precipitate out. The purified polymer was collected by filtration and dried under vacuum for 1 day to give a dark solid (143 mg, 46%, M_n = 7000, PDI = 1.86). ^{1}H NMR ($CDCl_3$, 300 MHz): δ = 0.50–1.45 (m, 60H), 1.90–2.30 (m, 8H), 7.20–7.70 (m, 8H), 7.80–8.25 ppm (m, 4H).

Acknowledgements

We thank the National Science Council and the ATU Program of the Ministry of Education, Taiwan, for financial support. We thank Prof. Ian Liao for the help with the AFM measurements.

[1] a) G. Yu, J. Gao, J. C. Hummelen, F. Wudl, A. J. Heeger, *Science* **1995**, *270*, 1789–1791; b) S. Günes, H. Neugebauer, N. S. Sariciftci, *Chem. Rev.* **2007**, *107*, 1324–1338; c) B. C. Thompson, J. M. J. Fréchet, *Angew. Chem.* **2008**, *120*, 62–82; *Angew. Chem. Int. Ed.* **2008**, *47*, 58–77; d) Y.-J. Cheng, S.-H. Yang, C.-S. Hsu, *Chem. Rev.* **2009**, *109*, 5868–5923.

[2] a) J. Roncali, *Chem. Rev.* **1997**, *97*, 173–206; b) H. A. M. van Mullekom, J. A. J. M. Vekemans, E. E. Havinga, E. W. Meijer, *Mater. Sci. Eng. R* **2001**, *32*, 1–40.

[3] a) Q. Zheng, B. J. Jung, J. Sun, H. E. Katz, *J. Am. Chem. Soc.* **2010**, *132*, 5394–5404; b) J.-S. Wu, Y.-J. Cheng, M. Dubosc, C.-H. Hsieh, C.-Y. Chang, C.-S. Hsu, *Chem. Commun.* **2010**, *46*, 3259–3261; c) Y. Liang, Z. Xu, J. Xia, S.-T. Tsai, Y. Wu, G. Li, C. Ray, L. Yu, *Adv. Mater.* **2010**, *22*, E135-E138; d) L. Huo, J. Hou, S. Zhang, H.-Y. Chen, Y. Yang, *Angew. Chem.* **2010**, *122*, 1542–1545; *Angew. Chem. Int. Ed.* **2010**, *49*, 1500–1503; e) N. Allard, R. B. Aïch, D. Gendron, P.-L. T. Boudreault, C. Tessier, S. Alem, S.-C. Tse, Y. Tao, M. Leclerc, *Macromolecules* **2010**, *43*, 2328–2333; f) N. Blouin, A. Michaud, M. Leclerc, *Adv. Mater.* **2007**, *19*, 2295–2300; g) E. Zhou, M. Nakamura, T. Nishizawa, Y. Zhang, Q. Wei, K. Tajima, C. Yang, K. Hashimoto, *Macromolecules* **2008**, *41*, 8302–8305; h) J. Hou, H.-Y Chen, S. Zhang, G. Li, Y. Yang, *J. Am. Chem. Soc.* **2008**, *130*, 16144–16145.

[4] a) M. Svensson, F. Zhang, S. C. Veenstra, W. J. H. Verhees, J. C. Hummelen, J. M. Kroon, O. Inganäs, M. R. Andersson, *Adv. Mater.* **2003**, *15*, 988–991; b) Q. Zhou, Q. Hou, L. Zheng, X. Deng, G. Yu, Y. Cao, *Appl. Phys. Lett.* **2004**, *84*, 1653–1655; c) F. Zhang, E. Perzon, X. Wang, W. Mammo, M. R. Andersson, O. Inganäs, *Adv. Funct. Mater.* **2005**, *15*, 745–750; d) F. Zhang, W. Mammo, L. M. Andersson, S. Admassie, M. R. Andersson, O. Inganäs, *Adv. Mater.* **2006**, *18*, 2169–2173; e) L. H. Slooff, S. C. Veenstra, J. M. Kroon, D. J. D. Moet, J. Sweelssen, M. M. Koetse, *Appl. Phys. Lett.* **2007**, *90*, 143506–143509; f) F. Zhang, J. Bijleveld, E. Perzon, K. Tvingstedt, S. Barrau, O. Inganäs, M. R. Andersson, *J. Mater. Chem.* **2008**, *18*, 5468–5474; g) G. L. Schulz, X. Chen, S. Holdcroft, *Appl. Phys. Lett.* **2009**, *94*, 023302–023305; h) F. Huang, K.-S. Chen, H.-L. Yip, S. K. Hau, O. Acton, Y. Zhang, J. Luo, A. K.-Y. Jen, *J. Am. Chem. Soc.* **2009**, *131*, 13886–13887.

[5] P. Coppo, M. L. Turner, *J. Mater. Chem.* **2005**, *15*, 1123–1133 and references therein.

[6] a) Z. Zhu, D. Waller, R. Gaudiana, M. Morana, D. Mühlbacher, M. Scharber, C. Brabec, *Macromolecules* **2007**, *40*, 1981–1986; b) D. Mühlbacher, M. Scharber, M. M. Zhengguo, M. M. Z. Zhu, D. Waller, R. Gaudiana, C. Brabec, *Adv. Mater.* **2006**, *18*, 2884–2889; c) J. Y. Kim, K. Lee, N. E. Coates, D. Moses, T.-Q. Nguyen, M. Dante, A. J. Heeger, *Science* **2007**, *317*, 222–225; d) J. Peet, J. Y. Kim, N. E. Coates, W. L. Ma, D. Moses, A. J. Heeger, G. C. Bazan, *Nat. Mater.* **2007**, *6*, 497–500.

[7] J. Roncali, *Macromol. Rapid Commun.* **2007**, *28*, 1761–1775 and references therein.

[8] a) J. L. Brédas, J. P. Calbert, D. A. da Silva Filho, J. Cornil, *Proc. Natl. Acad. Sci. USA* **2002**, *99*, 5804–5809; b) S. Ando, J.-I. Nishida, H. Tada, Y. Inoue, S. Tokito, Y. Yamashita, *J. Am. Chem. Soc.* **2005**, *127*, 5336–5337; c) N.-S. Baek, S. K. Hau, H.-L. Yip, O. Acton, K.-S. Chen, A. K.-Y. Jen, *Chem. Mater.* **2008**, *20*, 5734–5736; d) Y. Liang, Y. Wu, D. Feng, S.-T. Tsai, H.-J. Son, G. Li, L. Yu, *J. Am. Chem. Soc.* **2009**, *131*, 56–57.

[9] a) K.-T. Wong, T.-C. Chao, L.-C. Chi, Y.-Y. Chu, A. Balaiah, S.-F. Chiu, Y.-H. Liu, Y. Wang, *Org. Lett.* **2006**, *8*, 5033–5036; b) S.-H. Chan, C.-P. Chen, T.-C. Chao, C. Ting, C.-S. Lin, B.-T. Ko, *Macromolecules* **2008**, *41*, 5519–5526; c) C.-P. Chen, S.-H. Chan, T.-C. Chao, C. Ting, B.-T. Ko, *J. Am. Chem. Soc.* **2008**, *130*, 12828–12833; d) C.-Y. Yu, C.-P. Chen, S.-H. Chan, G.-W. Hwang, C. Ting, *Chem. Mater.* **2009**, *21*, 3262–3269.

[10] a) P. Baierweck, U. Simmross, K. Müllen, *Chem. Ber.* **1988**, *121*, 2195–2200; b) J. Roncali, C. Thobie-Gautier, *Adv. Mater.* **1994**, *6*, 846–848; c) T. Kowada, T. Kuwabara, K. Ohe, *J. Org. Chem.* **2010**, *75*, 906–913.

[11] I. Afonina, S. J. Coles, M. B. Hursthouse, A. Kanibolotsky, P. J. Skabara, *Acta Crystallogr. Sect. E* **2008**, *64*, o167.

[12] a) A. F. Littke, C. Dai, G. C. Fu, *J. Am. Chem. Soc.* **2000**, *122*, 4020–4028; b) M. Ahlquist, P.-O. Norrby, *Organometallics* **2007**, *26*, 550–553.

[13] a) Q. Hou, Y. Xu, W. Yang, M. Yuan, J. Peng, Y. Cao, *J. Mater. Chem.* **2002**, *12*, 2887–2892; b) G. L. Schulz, S. Holdcroft, *Chem. Mater.* **2008**, *20*, 5351–5355; c) J. Hou, Z. Tan, Y. Yan, Y. He, C. Yang, Y. Li, *J. Am. Chem. Soc.* **2006**, *128*, 4911–4916; d) Y. Li, Y. Zou, *Adv. Mater.* **2008**, *20*, 2952–2958; e) E. Zhou, Z. Tan, Y. Yang, L. Huo, Y. Zou, C. Yang, Y. Li, *Macromolecules* **2007**, *40*, 1831–1837; f) Y. Liang, S. Xiao, D. Feng, L. Yu, *J. Phys. Chem. C* **2008**, *112*, 7866–7871; g) J. Hou, Z. Tan, Y. He, C. Yang, Y. Li, *Macromolecules* **2006**, *39*, 4657–4662; h) Q. Peng, K. Park, T. Lin, M. Durstock, L. Dai, *J. Phys. Chem. B* **2008**, *112*, 2801–2808.

[14] a) B. P. Rand, J. Genoe, P. Heremans, J. Poortmans, *Prog. Photovolt: Res. Appl.* **2007**, *15*, 659–676; b) T. Johansson, W. Mammo, M. Svensson, M. R. Andersson, O. Inganäs, *J. Mater. Chem.* **2003**, *13*, 1316–1323.

[15] a) M. M. Wienk, J. M. Kroon, W. J. H. Verhees, J. Knol, J. C. Hummelen, P. A. van Hal, R. A. J. Janssen, *Angew. Chem.* **2003**, *115*, 3493–3497; *Angew. Chem. Int. Ed.* **2003**, *42*, 3371–3375; b) Y. Yao, C. Shi, G. Li, V. Shrotriya, Z. Pei, Y. Yang, *Appl. Phys. Lett.* **2006**, *89*, 153507–153510.

[16] C.-H. Chen, C.-H. Hsieh, M. Dubosc, Y.-J. Cheng, C.-S. Hsu, *Macromolecules* **2010**, *43*, 697–708.

[17] a) H. Hoppe, N. S. Sariciftci, *J. Mater. Chem.* **2006**, *16*, 45–61; b) J. Liu, Y. Shi, Y. Yang, *Adv. Funct. Mater.* **2001**, *11*, 420–424.

[18] U. Scherf, A. Gutacker, N. Koenen, *Acc. Chem. Res.* **2008**, *41*, 1086–1097 and references therein.

Received: July 20, 2010
Published online: October 8, 2010

